PHYSICAL REVIEW B VOLUME 51, NUMBER 19 15 MAY 1995-I

Density-functional calculation of the bulk and surface geometry of beryllium

N. A. W. Holzwarth and Y. Zeng

Department of Physics, Wake Forest University, Winston–Salem, North Carolina 27109

(Received 19 October 1994)

The equilibrium lattice parameters and elastic consants of bulk Be and the optimized geometry of the Be (0001) surface were studied using density-functional theory and mixed-basis pseudopotential techniques. Results obtained with various forms of the exchange-correlation functional are compared, including the local-density approximation (LDA) and the generalized-gradient approximation (GGA). For the bulk Be, the GGA results are slightly closer to the experimental values than are the LDA results. However, for the Be (0001) surface, neither the GGA nor LDA results explain the anomalously large expansion of the top layer observed in experimental low-energy electron-diffraction data.

I. INTRODUCTION

The simple metal, beryllium, having the hexagonal-close-packed structure and the largest average valence electron density,[1] has been the subject of extensive theoretical and experimental study. From the point of view of theoretical solid-state physics, Be metal has the role that He takes in theoretical atomic physics. Consequently, there is a strong motivation to understand the physical and/or numerical reasons for relatively small discrepancies between theory and experiment.

In a recent paper, Davis and co-workers[2] analyzed the low-energy electron-diffraction (LEED) spectra for a Be (0001) surface, finding that the equilibrium geometry of the surface layer corresponds to a 5.8% expansion relative to the bulk layer spacing. This is an unusually large expansion in comparison with other known surfaces,[2] including that of the chemically and structurally related material Mg (0001), which was recently found[3] to have a surface layer expansion of only 1.9%. Density functional calculations of the anomalous surface layer expansion of Be (0001) have been performed by Feibelman,[4] using the local-density approximation with the correlation functional of Wigner.[5] In the present work, we extend this study to consider the effects of the form of the exchange-correlation functional on the calculated surface layer expansion of Be (0001), including the use of the generalized gradient approximation of Perdew and co-workers[6] (GGA or GGA-PW91). The GGA-PW91 has been shown to improve the agreement between calculated and experimental equilibrium properties of a number of materials.[6–8]

The outline of this paper is as follows. In Sec. II, the calculational methods are briefly detailed. In Sec. III, results for the bulk calculations are presented. In Sec. IV, the surface relaxation results are presented. In Sec. V, the results are summarized and discussed.

II. CALCULATIONAL METHODS

The calculational methods used in the present work are very similar to those used by many other groups as reviewed by Pickett[9] as detailed in a previous paper.[7] Briefly, the calculations are based on density-functional theory,[10] within the frozen-core approximation, implemented using norm-conserving pseudopotentials[11] and a mixed-basis representation of the electronic wave functions.[12] The calculational parameters that determine the calculational efficiency and accuracy are as follows. The pseudopotential matching radii r_l were chosen to be 2.1 bohr for both $l=0$ and $l=1$. The reciprocal-lattice range parameters were chosen to be $Q_{\max}=12$ bohr^{-1} the converging Hamiltonian matrix elements, $|q_{\mathrm{PW}}|^2=12$ bohr^{-2} for representing the plane-wave component of the wave functions, and $|q_{\mathrm{LCAO}}|^2=49$ bohr^{-2} for representing the linear-combination-of-atomic-orbital component of the wave functions. The convergence of the density self-consistency was taken to be $\Delta_\rho \equiv \sum_{\mathbf{G}} |\rho^{\mathrm{out}}(\mathbf{G})-\rho^{\mathrm{in}}(\mathbf{G})| \leq 5\times10^{-6}$ bohr^{-3}/atom. The number of inequivalent **k** points Brillouin-zone sampling were taken to be 150 for the bulk calculations and 55 for the surface calculations. The Gaussian smoothing parameter, $\sigma=0.2$ eV, was used to approximate integrals over the Brillouin zone.[13] These parameters were chosen to ensure that the calculations were very well converged.

For each assumed geometry, the self-consistent cohesive energy E_{coh} is calculated as the difference between the valence electron energy of the atom, E_{atom}, and that the solid,[14] which is comprised of the ion-ion (Ewald) energy E_{Ewald}, the one-electron energy E_{one}, the electron-electron repulsion correction energy E_{Coul}, and the exchange-correlation energy term E_{xc} (which includes both the conventional exchange-correlation energy, as well as the appropriate correction to E_{one}):

$$E_{\mathrm{coh}}=E_{\mathrm{atom}}-(E_{\mathrm{Ewald}}+E_{\mathrm{one}}+E_{\mathrm{Coul}}+E_{\mathrm{xc}}) \ . \tag{1}$$

In this work, several forms of the exchange-correlation functional were used. Within the local-density approximation, we used the correlation functional based on the Monte Carlo calculations for the free-electron gas by Ceperley and Alder[15] as fit by Perdew and Wang[16] (LDA or LDA-CA). In addition, gradient corrections were considered using the generalized gradient approximation (GGA-PW91) designed by Perdew and co-workers.[6] Finally, in order to compare with the work of Feibelman,[4] we also performed local-density approximation calculations using Wigner's interpolation formula.[5]

0163-1829/95/51(19)/13653(7)/$06.00

In this work, since we are concerned with systems with few degrees of freedom, it is convenient to perform the calculation for a grid of possible geometries and to use polynomial interpolation to estimate the optimal energy and the elastic coefficients. For the bulk lattice, the cohesive energy is a function of the two lattice parameters a and c and can be conveniently fit to the quadratic form:[17]

$$\begin{aligned} E_{\mathrm{coh}}(a,c)=E_{\mathrm{coh}}(a_0,c_0)&+\tfrac{1}{2}(a-a_0)^2\frac{\partial^2 E_{\mathrm{coh}}}{\partial a^2}\\ &+\tfrac{1}{2}(c-c_0)^2\frac{\partial^2 E_{\mathrm{coh}}}{\partial c^2}\\ &+(a-a_0)(c-c_0)\frac{\partial^2 E_{\mathrm{coh}}}{\partial a\,\partial c}\ . \end{aligned} \tag{2}$$

By minimizing the χ^2 function for this fitting function with the weight factor

$$W(a,c)=\frac{1}{(a-a_0)^2+(c-c_0)^2+\epsilon}\ , \tag{3}$$

the equilibrium lattice parameters a_0 and c_0 and the corresponding energy derivatives

$$\frac{\partial^2 E_{\mathrm{coh}}(a_0,c_0)}{\partial a^2}\ ,\quad \frac{\partial^2 E_{\mathrm{coh}}(a_0,c_0)}{\partial c^2}\ ,$$

and

$$\frac{\partial^2 E_{\mathrm{coh}}(a_0,c_0)}{\partial a\,\partial c}\ ,$$

can be determined accurately. In Eq. (3), ϵ represents a small positive parameter, which was introduced in order to emphasize the calculational results near the equilibrium geometry without destabilizing the fitting procedure.[18] Once these parameters are determined, the elastic constants can be directly calculated using the relations:

$$c_{11}+c_{12}=-\frac{a_0^2}{2V_0}\frac{\partial^2 E_{\mathrm{coh}}}{\partial a^2}\ , \tag{4}$$

$$c_{33}=-\frac{c_0^2}{V_0}\frac{\partial^2 E_{\mathrm{coh}}}{\partial c^2}\ , \tag{5}$$

$$c_{13}=-\frac{a_0c_0}{2V_0}\frac{\partial^2 E_{\mathrm{coh}}}{\partial a\,\partial c}\ , \tag{6}$$

$$B=-\frac{1}{9V_0}\left[a_0^2\frac{\partial^2 E_{\mathrm{coh}}}{\partial a^2}+c_0^2\frac{\partial^2 E_{\mathrm{coh}}}{\partial c^2}+2a_0c_0\frac{\partial^2 E_{\mathrm{coh}}}{\partial a\,\partial c}\right]. \tag{7}$$

In the above expressions, V_0 denotes the equilibrium volume per atom.

For the surface calculations, a supercell geometry was used, including nine layers of the Be lattice and three empty layers (approximately 7 Å) representing the vacuum. (Calculations using five empty layers to represent the vacuum gave essentially the same results.) Fixing the intralayer lattice constant and the spacing between interior layers to correspond to the optimal bulk values a_0 and c_0, the cohesive energy was optimized with respect to the spacing between the outer most layers. Both outer sur-

TABLE I. Comparison of structural and elastic properties of bulk beryllium.

	Present calculations			Previous calculations				
	GGA	LDA	Wigner	Dovesi[a]	Chou[b]	Blaha[c]	Feibelman[d]	Exp.
a (Å)	2.25	2.23	2.26	2.32	2.25	2.24	2.27	2.29[e]
c (Å)	3.54	3.51	3.56	3.64	3.57	3.54	3.59	3.58[e]
c/a	1.57	1.58	1.57	1.57	1.59	1.58	1.58	1.57[e]
E_{coh} (eV/atom)[f]	3.65	4.08	3.82	1.73	3.60	3.9		3.32[g]
B (10^{11} Pa)	1.2	1.4	1.2		1.4	1.3	1.2	1.1[h]
$c_{11}+c_{12}$ (10^{11} Pa)	3.5	3.9	3.5		4.0	3.5	3.4	3.1[h] 3.2[i]
c_{33} (10^{11} Pa)	3.9	4.2	3.9		3.8	4.4	3.7	3.5[h] 3.6[i]
c_{13} (10^{11} Pa)	−0.03	0.1	0.03		0.2	0.03	0.07	0.5[h] −0.01[i]

[a] Reference 21, using Hartree-Fock formalism (with no correlation contribution).

[b] Reference 17, using Hedin-Lundqvist correlation functional with pseudopotential formalism; elastic constant parameters inferred from author's fit to functional form of Eq. (2).

[c] Reference 22, using Hedin-Lundqvist correlation functional with LAPW formalism; elastic constant parameters inferred from author's fit to functional form of Eq. (2).

[d] Reference 4, using Wigner correlation functional; quoted energy results refit to weighted quadratic form [Eqs. (2)–(7)].

[e] Reference 23.

[f] Each calculated cohesive energy has been normalized per atom and has been corrected for the estimated (Ref. 17) zero-point energy of 0.14 eV/atom.

[g] Reference 24.

[h] Reference 25.

[i] Reference 26.

faces of the model film were relaxed at the same time, in order to maintain the mirror symmetry of the supercell. For each geometry, the surface energy per surface atom was estimated from[4]

$$E_{\text{surf}}=\tfrac{1}{2}\{9E_{\text{coh}}(\text{bulk})-E_{\text{coh}}(\text{9-layer film})\}\ . \tag{8}$$

In this expression, the two terms in the brackets represent the cohesive energy of the nine-layer film subtracted from that of an equal number of bulk atoms. The difference is divided by two, because the supercell has two equivalent surfaces. In general, the surface energy is positive, indicating the greater stability of the bulk crystal than that of the surface. Several authors[19,20] have pointed out that E_{surf} calculated in this way is sensitive to the film thickness. However, in this work, we focus on studying E_{surf} as a function of relaxation for fixed film thickness.

III. RESULTS FOR BULK BERYLLIUM

The properties of bulk Be have been very well studied both theoretically and experimentally. For example, theoretical studies have been carried out within Hartree-Fock theory by Dovesi and co-workers[21] and within density-functional LDA theory by Chou and co-workers,[17] using pseudopotential techniques and by Blaha and Schwarz[22] using full potential linearized-augmented-plane-wave (LAPW) techniques. The results of these studies are in very good agreement with experimental data, including structural and elastic parameters,[23–26] as well as x-ray-diffraction data.[27] In preparation for our surface studies, we have recalculated the structural and elastic properties of bulk Be. The results are summarized in Table I in comparison with previous calculations and experimental measurements. This table shows that the results are more sensitive to the form of the exchange-correlation formalism than to the calculational techniques. In general, the LDA calculations, including the present work using the Ceperley-Alder-Perdew-Wang[16] correlation functional and the earlier work of Chou and co-workers[17] and of Blaha and Schwarz,[22] using the Hedin-Lundqvist correlation formula,[28] underestimate the bulk lattice constants, while overestimating the cohesive energy and elastic coefficients. The GGA-PW91 calculation results are generally closer to the experimental values as are those obtained using the Wigner interpolation formula, both in the present work and in that of Feibelman.[4] The pure Hartree-Fock results of Dovesi and co-workers[21] overestimate the bulk lattice constants and substantially underestimate the cohesive energy, indicating that correlation effects are substantial.

The self-consistent valence pseudodensity $\rho(\mathbf{r})$ of crystalline Be is a by product of these calculations. This is most conveniently represented in terms of the deformation density $\Delta\rho(\mathbf{r})$, which can be calculated from the difference between $\rho(\mathbf{r})$ and the superposed valence pseudodensity of Be atoms. This is shown in Fig. 1, comparing the GGA-PW91 and LDA-CA results in two perpendicular planes. Because these contour plots represent the deformation *pseudodensity*, the integral but not the shape of the charge density is correctly given in the core region of each atomic site; while both the integral and the shape of the charge density is accurately represented in the bonding and interstitial regions of the solid. From these plots, it is apparent that the GGA-PW91 and LDA-CA densities are very similar for bulk Be. The contours of the deformation density show a charge excess in the tetrahedral sites near each Be atom and a charge deficit

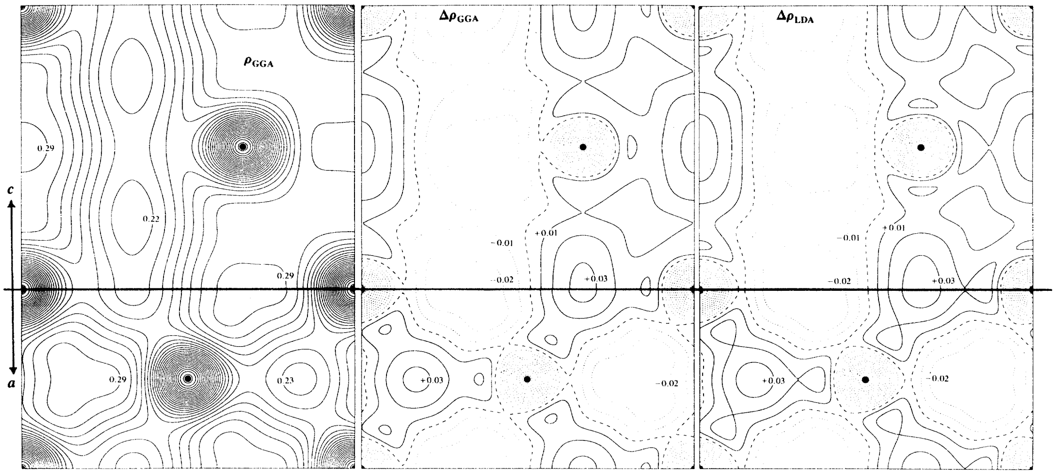

FIG. 1. Contour plots of the valence charge density of bulk Be plotted in two perpendicular planes. The lower panels, indicated with an arrow pointing in the a direction, plot the density in the a hexagonal layer plane. The upper panels, indicated with an arrow pointing in the c direction, plot the density in an intersecting plane containing the c axis. The atomic positions are indicated with filled circles. Contour levels are drawn at multiples of 0.01 electrons/Å^3. The left panel, labeled ρ_{GGA}, represents the contours calculated using the GGA-PW91 exchange-correlation functional; the middle and right panels, labeled $\Delta\rho_{\text{GGA}}$ and $\Delta\rho_{\text{LDA}}$, represent the deformation density for bulk Be comparing the results for the GGA-PW91 and LDA-CA functions, respectively. Positive contours are drawn with a solid line, negative contours are drawn with a dotted line, and the zero contour is drawn with a dashed line.

in the octahedral holes. This directional bonding was characterized by Yang and Coppens[2] in terms of sp^2 hybrid orbitals forming trigonal bonds in each Be layer and sp hybrid orbits forming bonds between the layers. The trigonal structure of the deformation density within the hexagonal layer, characteristic of sp^2 hybridization, and the excess charge between the layers, characteristic of sp hybridization, are consistent with these deformation density plots. The fact that there is interlayer bonding, characterized by significant excess charge between the layers, is consistent with the fact that the c/a ratio for Be, 1.57, is significantly smaller than the ideal c/a ratio of 1.63. These qualitative features of the deformation density are consistent with experimental data[27,29] and previous calculations.[21,17,22,30]

IV. SURFACE RELAXATION STUDIES

In studying the surface relaxation of Be (0001), we focused on the relaxation of the outer most layer; since, according to the work of Feibelman[4] and Stumpf and Feibelman,[31] the relaxation of the inner layers contributes a very small percentage of the total relaxation energy (roughly 0.002 eV/surface atom). The geometry optimization results are summarized in Fig. 2 and Table II. In Fig. 2, the surface energy per surface atom [Eq. (8)] is plotted, with respect to the fractional change in the outer most layer spacing $\Delta d_{12}/d_{12}^{\rm bulk}$, where $d_{12}^{\rm bulk} \equiv c_0/2$ is the bulk layer spacing. The three curves represent the present work, using the LDA-CA, GGA-PW91, and Wigner correlation functionals, respectively. In addition to quantifying the surface relaxation in terms of the fractional change in the layer separation, $\Delta d_{12}/d_{12}^{\rm bulk}$, another way of describing the same quantity is in terms of the effective c/a ratio of the surface layer: $(c/a)_{\rm surf} \equiv 2d_{12}/a_0$. These are listed in Table II along with the corresponding values of the fractional change in the layer separation.

The results of the present work shows that the relaxation of the surface layer of Be (0001) varies between 2.1% and 2.5% depending upon the exchange-correlation functional. This is considerably smaller than the relaxation calculated in the earlier work of Feibelman[4] and others,[32,33] as well as smaller than the relaxation determined from LEED measurements.[2] As quoted in Table II, recent calculations by Stumpf and Feibelman,[31] using the LDA with the Ceperley-Alder correlation functional[15] and with better Brillouin zone sampling than the earlier work of Feibelman,[4] are consistent with our results. For a multilayer optimization, Stumpf and Feibelman[31] find $\Delta d_{12}/d_{12}^{\rm bulk} = 2.7\%$; while, if only the outer layer is relaxed, $\Delta d_{12}/d_{12}^{\rm bulk} \approx 2\%$. These first-principles results are different from the empirical potential results of Antonelli and co-workers[32] and of Chen,[33] indicating that electronic excitation effects may be important.

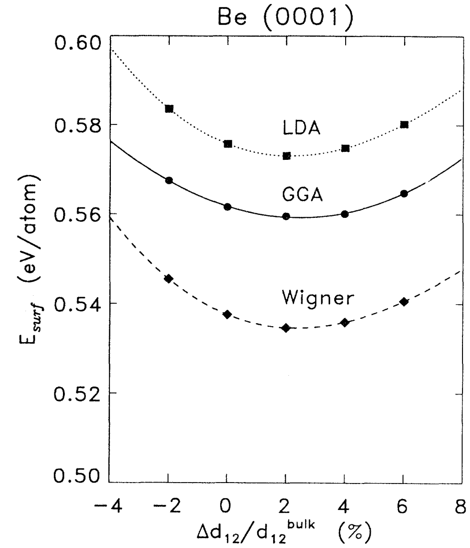

FIG. 2. Plot of $E_{\rm surf}$ as defined in Eq. (8) versus fractional change in layer spacing for nine-layer Be thin films calculated in the present work using LDA-CA (■), GGA-PW91 (●), and Wigner (◆) forms of the exchange-correlation functional. Calculated values correspond to relaxation of surface layer only and are indicated with solid symbols connected with least-squares fitted polynomial functions.

TABLE II. Comparison of results for relaxation of the Be (0001) surface.

	$(c/a)_{\rm surf}$	$\Delta d_{12}/d_{12}^{\rm bulk}$	$\Delta d_{23}/d_{23}^{\rm bulk}$	$\Delta d_{34}/d_{34}^{\rm bulk}$
Present work: GGA-PW91	1.62	+2.5%		
Present work: LDA-CA	1.61	+2.1%		
Present work: Wigner	1.61	+2.3%		
Stumpf and Feibelman[a]	1.61	+2.7%	+1.2%	+0.6%
Feibelman[b]	1.65	+3.9%	+2.2%	
Many-body effective potential from LDA cluster calculations[c]	1.73	+5.9%	+0.9%	+0.0%
Local volume empirical potential[d]	1.70	+4.1%	+0.5%	+0.3%
Experiment[e]	1.66	+5.8%	−0.2%	+0.2%

[a] Reference 31 (LDA-CA).
[b] Reference 4 (Wigner).
[c] Reference 32; bulk $c/a \approx 1.63$.
[d] Reference 33; bulk $c/a \equiv 1.63$.
[e] Reference 2.

For our LDA-CA and GGA-PW91 results, we find a minimum surface energy of 0.573 eV/atom and 0.559 eV/atom, corresponding to a surface relaxation of 2.1% and 2.5% and an effective surface c/a ratio of 1.61 and 1.62, respectively. Both of these calculations indicate that the surface layer c/a ratio of Be expands from its contracted bulk value of 1.57 to nearly the ideal value of 1.63 at the surface layer. The calculations give the same trend as the experimental results, but predict a much smaller magnitude of the effect. This trend can be described in terms of a change in the bond hybridization near the surface layer, or as described by Feibelman,[4] a decrease in the p-like character of the states near the surface.

In order to visualize these effects, it is helpful to see the charge contours of the valence electrons. In Fig. 3, the contours for the GGA-PW91 valence pseudocharge are presented, comparing contours for the unrelaxed lattice with those for the $\Delta d_{12}/d_{12}^{\mathrm{bulk}}=2\%$ lattice. The contours for the two surface geometries are very similar to each other and also similar to the corresponding results presented by Feibelman,[4] for the Wigner correlation functional. In these plots, it is apparent that the charge density achieves nearly planar contours in the vicinity of the surface. In the last panel of Fig. 3, the difference between the charge density of the relaxed and unrelaxed surfaces is presented. The magnitude of the difference is less than 3% of the valence density and is localized near the surface. Not surprisingly, it generally corresponds to charge flowing out of the surface as the surface expands. However, in the immediate vicinity of each surface atom, the charge flows in the opposite direction.

Further surface effects are seen more clearly in Fig. 4, which shows a plot of the deformation density and a plot of the difference between the surface density and the bulk density for the unrelaxed GGA-PW91 calculation. The deformation density plot shows that at the surface plane, a charge builds up in mostly at the sites corresponding to the bulk tetrahedral holes, but also at the sites corresponding to the bulk octahedral holes. Qualitatively similar results were seen in the Hartree-Fock results for a four-layer unrelaxed Be film by Angonoa, Koutecky, and Pisani.[34] The surface effects are seen more clearly in the plot of the difference between the surface density and that of the bulk lattice. There is a region of positive contours at the surface site corresponding to the bulk octahedral holes and negative contours having the shape of sp hybrid density below each surface atom. This difference density is essentially zero below the third layer.

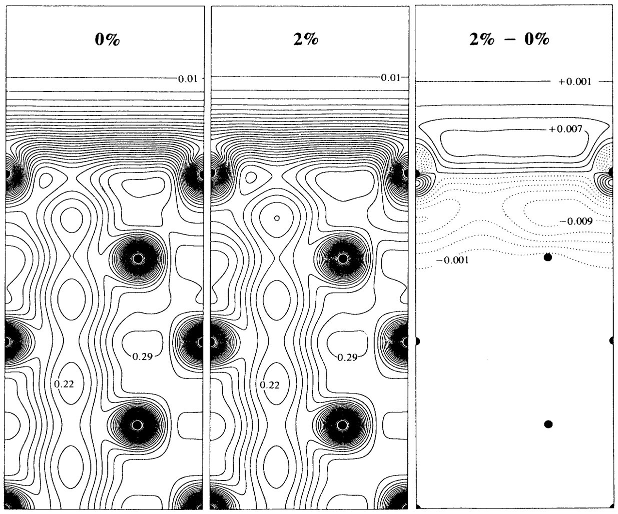

FIG. 3. Contour plots of the GGA-PW91 valence charge density for Be (0001) plotted in the plane containing the c axis, in the first two panels comparing the results of the unrelaxed (0%) surface with that of $\Delta d_{12}/d_{12}^{\mathrm{bulk}}=2\%$, with contour levels drawn at multiples of 0.01 electrons/Å^3. The right panel shows the contours of the difference between the density of the expanded lattice minus that of the reference lattice, with contour levels drawn at odd multiples of 0.001 electrons/Å^3. Positive contours are drawn with a solid line, negative contours are drawn with a dotted line. The atomic positions are indicted with filled circles.

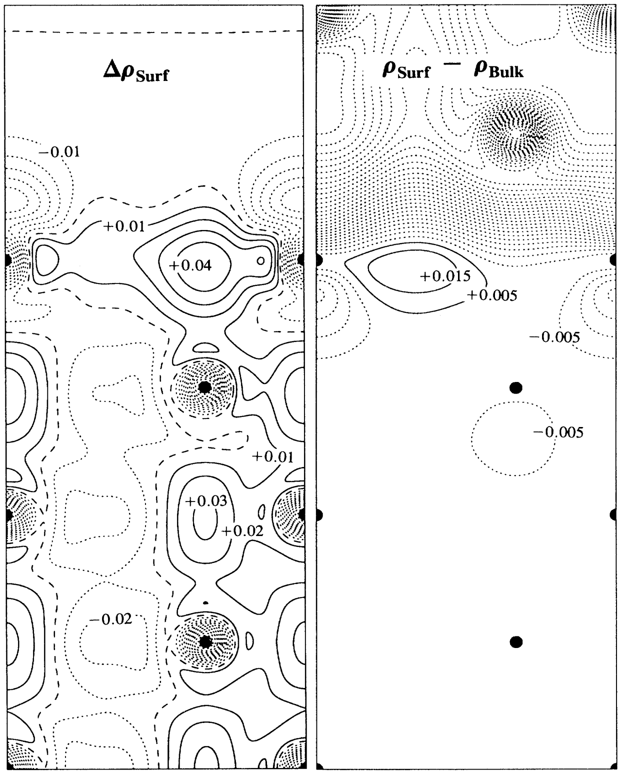

FIG. 4. Contour plots of the GGA-PW91 valence charge density for unrelaxed Be (0001) plotted in the plane containing the c axis, comparing the deformation density (left panel with contour levels drawn at multiples of 0.01 electrons/Å^3) and the difference between the self-consistent surface density and that of the bulk crystal (right panel with contour levels drawn at intervals of 0.01 electrons/Å^3, shifted by 0.005 electrons/Å^3). Positive contours are drawn with a solid line, negative contours are drawn with a dotted line, and zero contour is drawn with a dashed line. The atomic positions are indicated with filled circles.

We also studied the surface band dispersion for this system. The surface bands of Be (0001) have been carefully mapped by Ray, Pan, and Plummer[35] and reviewed by Plummer and Hannon.[36] We find the surface band structure to be very insensitive to the relaxation and to be in good agreement with experiment[35,36] and previous calculations.[4,37] In particular, there is an occupied surface band a few eV below the Fermi level within most of the surface band gap of Be (0001). Near the $\overline{M}$ point and along the $\overline{M}$-$\overline{K}$ direction, there are two surface bands;[37,36] the lower band having a peak density in the third layer and being barely distinguishable in our nine-layer slab calculation.

V. DISCUSSION AND SUMMARY

We have shown that density-functional calculations, using pseudopotential techniques, are able to reproduce the experimentally observed[2] expansion of the surface layer of Be (0001) crystals qualitatively, but not quantitatively. The results are sensitive to the form of the exchange-correlation functional; however, the GGA-PW91 functional produces only small changes relative to the LDA-CA functional, and is not able to account for the discrepancy with experiment. There are a number of possible reasons for this discrepancy. One possibility, is the contribution of core-electron effects. In the pseudopotential formulation, the core electrons are assumed to be frozen at the atomic densities. In LAPW studies of bulk Be, Blaha and Schwarz[22] found the core density expansion to be about 0.1–0.3%. Recent high-resolution photoemission studies of the Be (0001) surface[38] have identified four distinct Be 1*s* peaks identified with the three nearest surface layers and the bulk. Early theoretical calculations were able to approximately reproduce these experimental results without considering structural relaxation and more recent calculations[39] have shown that surface relaxations have a very small effect on the core-level shifts. However, it is still possible that the small changes in the core density exhibited by these surface core-level shifts can affect the energy and the structural relaxation of this system. As shown in Fig. 2, the energy minimum is very shallow and can be easily shifted by small contributions. Another possibility is image potential[40] effects. This classical effect is notoriously not included in the LDA and is very poorly included in the GGA. Although a detailed description of this effect in the vicinity of the surface is not available, its qualitative features are well known. In particular, the image potential tends to lower the potential near the surface barrier. This would enable the electrons to extend further toward the vacuum and thus to stabilize the layer expansion. Both of these effects should be studied in future work.

ACKNOWLEDGMENTS

This work was supported by NSF Grant No. DMR-8918712 and the North Carolina Supercomputer Center and benefited from conversions with Professor M.-Y. Chou, Professor E. W. Plummer, Dr. H. Davis, Dr. P. Feibelman, and Dr. R. Stumpf. We would also like to thank J. Perdew for sending us a copy of his GGA subroutines.

---

[1] N. W. Ashcroft and N. David Mermin, *Solid State Physics* (Saunders College, Philadelphia, 1976).

[2] H. L. Davis, J. B. Hannon, K.B. Kay, and E. W. Plummer, Phys. Rev. Lett. **68**, 2632 (1992).

[3] P. T. Sprunger, K. Pohl, H. L. Davis, and E. W. Plummer, Surf. Sci. **297**, L48 (1993).

[4] P. J. Feibelman, Phys. Rev. B **46**, 2532 (1992).

[5] E. Wigner, Phys. Rev. **46**, 1002 (1934).

[6] J. P. Perdew, J. A. Chevary, S. H. Vosko, K. A. Jackson, M. R. Pederson, D. J. Singh, and C. Fiolhais, Phys. Rev. B **46**, 6671 (1992).

[7] N. A. W. Holzwarth and Y. Zeng, Phys. Rev. **49**, 2351 (1994).

[8] Changyol Lee, David Vanderbilt, Kari Laasonen, R. Car, and M. Parrinello, Phys. Rev. B **47**, 4863 (1993).

[9] W. E. Pickett, Comput. Phys. Rep. **9**, 115 (1989).

[10] P. Hohenberg and W. Kohn, Phys. Rev. **136**, B864 (1964); W. Kohn and L. J. Sham, *ibid*. **140**, A1133 (1965).

[11] G. P. Kerker, J. Phys. C **13**, L189 (1980); N. Troullier and J. L. Martins, Phys. Rev. B **43**, 1993 (1991).

[12] S. G. Louie, K.-M. Ho, and M. L. Cohen, Phys. Rev. B **19**, 1774 (1992).

[13] C.-L. Fu and K.-M. Ho, Phys. Rev. B **28**, 5480 (1983).

[14] J. Ihm, A. Zunger, and M. L. Cohen, J. Phys. C **12**, 4409 (1979); **13**, 3095 (1980); J. Ihm, Rep. Prog. Phys. **51**, 105 (1988).

[15] D. M. Ceperley and B. J. Alder, Phys. Rev. Lett. **45**, 566 (1980).

[16] J. P. Perdew and Y. Wang, Phys. Rev. B **45**, 13 244 (1992).

[17] M. Y. Chou, P. K. Lam, and M. L. Cohen, Solid State Commun. **42**, 861 (1982); Phys. Rev. B **28**, 4179 (1983); **28**, 1696 (1983).

[18] The fit was assumed to be stable when the calculated coefficients were the same for $\epsilon = 10^{-8}$ bohr^2 and 10^{-9} bohr^2.

[19] P. J. Feibelman and D. R. Hamann, Phys. Rev. B **29**, 6463 (1984).

[20] J. C. Boettger, Phys. Rev. B **49**, 16 798 (1994).

[21] R. Dovesi, C. Pisani, F. Ricca, and C. Roetti, Phys. Rev. B **25**, 3731 (1982); Z. Phys. B **47**, 19 (1982).

[22] P. Blaha and K. Schwarz, J. Phys. F **27**, 899 (1987).

[23] R. Ferro, in *Beryllium: Physico-chemical Properties of Its Compounds and Alloys,* edited by O. Kubaschewski, Special Issue of At. Energy Rev. **4**, 63 (1973).

[24] Charles Kittel, *Introduction to Solid State Physics,* 6th ed. (Wiley, New York, 1986).

[25] W. D. Rowland and J. S. White, J. Phys. F **2**, 231 (1972).

[26] D. J. Silversmith and B. L. Averbach, Phys. Rev. B **1**, 567 (1970).

[27] N. K. Hansen, J. R. Schneider, and F. K. Larsen, Phys. Rev. B **29**, 917 (1984); F. K. Larsen and N. K. Hansen, Acta Crystallogr. Sect. B **40**, 169 (1984).

[28] L. Hedin and B. I. Lundqvist, J. Phys. C **4**, 2064 (1971).

[29] Y. W. Yang and P. Coppens, Acta Crystallogr. Sect. A **34**, 61 (1978).

[30] L. Massa, M. Goldberg, C. Frishberg, R. F. Boehme, and S. J. La Placa, Phys. Rev. Lett. **55**, 622 (1985).

[31] R. Stumpf and P. Feibelman (to be published).

[32] A. Antonelli, S. N. Khanna, and P. Jena, Surf. Sci. **289**, L614 (1993).

[33] S. P. Chen, Surf. Sci. **264**, L162 (1992).

[34] G. Angonoa, J. Koutecky, and C. Pisani, Surf. Sci. **122**, 355 (1982).

[35] K. B. Ray, X. Pan, and E. W. Plummer, Surf. Sci. **285**, 66 (1993).

[36] E. W. Plummer and J. B. Hannon, Prog. Surf. Sci. **46**, 149 (1994).

[37] E. V. Chulkov, V. M. Silkin, and E. N. Shirykalov, Surf. Sci. **188**, 287 (1987).

[38] L. I. Johansson, H. I. P. Johansson, J. N. Andersen, E. Lundgren, and R. Nyholm, Phys. Rev. Lett. **71**, 2453 (1993); M. Aldén, H. L. Skriver, and B. Johansson, *ibid.* **71**, 2457 (1993).

[39] P. J. Feibelman and R. Stumpf, Phys. Rev. B **50**, 17 480 (1994).

[40] D. Straub and F. J. Himpsel, Phys. Rev. B **33**, 2256 (1986).